DRAFT VERSION FEBRUARY 7, 2007
Preprint typeset using LaTeX style emulateapj v. 11/26/03

SWIFT OBSERVATIONS OF A FAR UV LUMINOSITY COMPONENT IN SS433

J. F. DOLAN[1,2], P. T. BOYD[2], J. K. CANNIZZO[2,3]

Draft version February 7, 2007

ABSTRACT

SS433 is a binary system showing relativistic Doppler shifts in its two sets of emission lines. The origin of its UV continuum is not well established. We observed SS433 to determine the emission mechanism responsible for its far UV spectrum. The source was observed at several different phases of both its 13 d orbital period and 162.5 d precession period using the UVOT and XRT detector systems on *Swift*. The far UV spectrum down to 1880 Å lies significantly above the spectral flux distribution predicted by extrapolating the reddened blackbody continuum that fits the spectrum above 3500 Å. The intensity of the far UV flux varies over a period of days and the variability is correlated with the variability of the soft X-ray flux from the source. An emission mechanism in addition to those previously detected in the optical and X-ray regions must exist in the far UV spectrum of SS433.

Subject headings: stars: individual: SS433 ultraviolet: stars X-rays: binaries

1. INTRODUCTION

SS433 is a binary system showing two sets of emission lines (Stephenson & Sanduleak 1977). The two emission line systems exhibit relativistic Doppler shifts in opposite directions corresponding to a mass motion velocity $v/c = 0.26$ (Margon 1984). The two sets of lines vary regularly in redshift with a 162.5 d period ascribed to the precession of two counter-directed beams. We adopt here the phase of Margon & Anderson (1989): $E(\psi)$ =JD$(2443562.37 \pm 0.30) + (162.50 \pm 0.03)\psi$, where $E(\psi)$ is the epoch at which the two sets of lines have the same redshift at integer values of ψ. The lines have a maximum redshift separation at phase $\psi = 0.631$. A smaller maximal separation occurs at $\psi = 0.131$, and a second epoch of redshift equality at $\psi = 0.262$. The system also exhibits a 13 d period in photometric and spectroscopic observations. The 13 d period is attributed to orbital motion and eclipse phenomena in the binary (Cherepashchuk 1981; Stewart et al 1987). We adopt here the 13 d phase φ of Goranskii et al. (1998) relative to photometric minimum at integer values of φ: $E(\varphi)$ =JD$(2450023.62 \pm 0.26) + (13.08211 \pm 0.00008)\varphi$.

Observations of SS433 in the radio show jet-like linear structure on both sides of the central radio source, which is coincident with the optical image (Hjellming & Johnston 1981; Neill et al. 1981). The position angle of the jets varies approximately sinusoidally with the 162.5 d precession period about a mean value of 100° ± 2° with amplitude 19° ± 3°. The radio emitting material appears to propagate away from the central source in discrete packets. VLBI observations have established that these "blobs" possess the same velocity as those producing the redshifted emission lines and give a distance to the source of 4.85 ± 0.2 kpc (Vermeulen et al. 1993).

The X-ray emission in SS433 originates near the base of the jets, which adiabatically expand and cool (Marshall et al. 1979; Brinkman et al. 1991; Kotani et al. 1996). The X-ray luminosity is $\sim 10^{36}$ erg s^{-1}. The spectrum between 1 and 10 keV shows multiple emission lines from several different species of highly ionized elements superposed on a continuum (Marshall et al. 2002). Marshall et al. modeled the continuum between 8 and 0.8 keV as a single power law with absorption,

$$\frac{dn}{dE} = 0.015E^{-1.35}e^{-\sigma(E)N_H} \text{ photons cm}^{-2}\text{ s}^{-1}\text{ keV}^{-1}, \quad (1)$$

where $N_H = 9.5 \times 10^{21}$ cm^{-2} is the hydrogen column density in the direction of SS433 and $\sigma(E)$ is the opacity of interstellar matter with normal cosmic abundances.

Spectra of SS433 from the infrared to the U band are acceptably represented by reddened blackbody emission (Gies et al. 2002) ascribed to the super-Eddington accretion disk around the compact object in the system and the dense part of an outflowing wind associated with the disk. UV observations with the High Speed Photometer (HSP) on the *Hubble Space Telescope* (*HST*) found excess emission above that predicted by extrapolating the reddened blackbody spectrum to 2770 Å (Dolan et al. 1997). Far UV observations of SS433 provide only upper limits on the flux between 1170 and 1575 Å (Gies et al. 2002) because of the large interstellar absorption along the line of sight. (SS433, at $l = 39°$, $b = -2°$, is highly reddened: $A_V = 7.8 \pm 0.5$ [Wagner 1986 and references cited therein]). This non-detection provides few significant constraints on the nature of any additional far-UV luminosity component. We therefore observed SS433 with the UV/Optical Telescope (UVOT) and X-Ray Telescope (XRT) on board the *Swift* satellite to confirm the existence of an additional luminosity component in the far UV. The observations might also locate the origin of this component in the binary system and constrain the physics of its emission mechanism.

2. OBSERVATIONS

The *Swift* mission, described by Gehrels et al. (2004), is devoted primarily to the detection of gamma-ray bursts and includes a UV/Optical telescope (UVOT) and an X-ray telescope (XRT) in its complement of instruments. The UVOT can observe photometrically in six different bandpasses centered between 1880 Å and the V band (cf. Table 1); its operation is described by Roming et al. (2005). The XRT is sensitive between 0.2 and 10 keV. Its operation is described by Burrows et al. (2005).

We observed SS433 with the UVOT and the XRT at the six epochs given in Table 2. The 13 d (orbital) phase and

[1] Department of Astronomy, San Diego State University San Diego, CA 92182-1221
[2] NASA/Goddard Space Flight Center, Exploration of the Universe Division, Greenbelt, MD 20771
[3] Joint Center for Astrophysics, University of Maryland, Baltimore County, Baltimore, MD 21250

TABLE 1. UVOT BANDPASSES

Filter Sensitivity	λ_c(Å)	FWHM(Å)	[a]	[b]
V	5440	750	2.24	220
B	4390	980	1.31	85
U	3450	875	1.49	60
UVW1	2510	700	3.52	75
UVM2	2170	510	6.89	110
UVW2	1880	760	6.04	70

[a]Inverse Sensitivity(1): 10^{-16} erg cm^{-2} s^{-1} Å^{-1}/(ct s^{-1})
[b]Inverse Sensitivity(2): μJy/(ct s^{-1})

TABLE 2. SS433 OBSERVATIONS

ID	(JD 2 453 000+)[a]	ψ[b]	φ[c]	V(mJy)[d]	UVW2(μJy)[e]
002	582.060	0.660	0.008	3.3(0.2)	<12.8
006	584.069	0.672	0.162	6.7(0.1)	7.2(3.7)
008	584.282	0.673	0.178	6.8(0.1)	9.0(2.7)
013A	600.544	0.773	0.426	5.7(0.1)	9.9(3.7)
013B	600.610	0.774	0.426	5.8(0.1)	6.0(3.9)
014	917.076	0.721	0.617	7.0(0.1)	3.7(1.2)
015	917.612	0.725	0.658	9.0(0.1)	13(1)
016	1043.300	0.498	0.265	9.0(0.1)	11(1)

[a]Start time
[b]Phase(Precessional)
[c]Phase(Orbital)
[d]Flux Density(1)
[e]Flux Density(2)

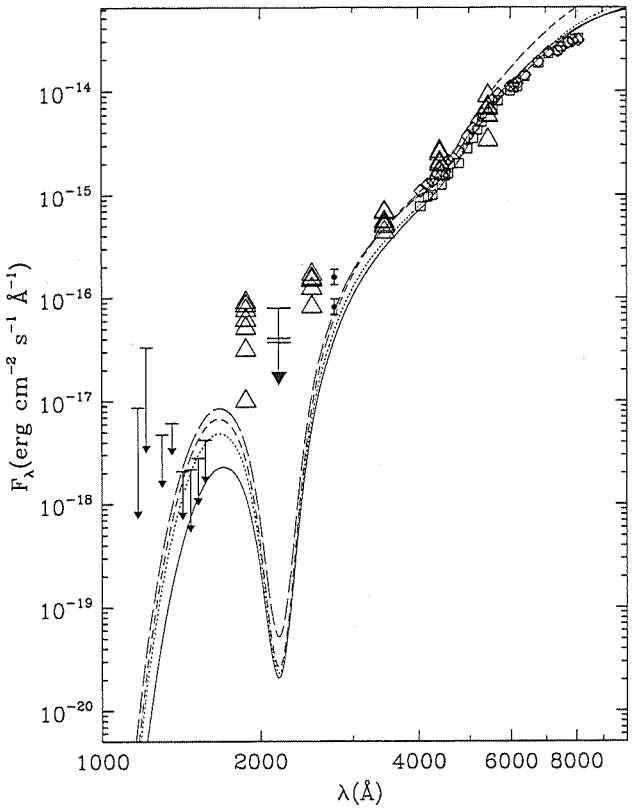

FIG. 1.— The spectral flux distribution observed from SS433. The data were taken at different epochs and different precessional and eclipse phases. Our individual UVOT observations for all visits in the six bandpasses given in Table 1 are shown as open triangles, except for the UVM2 data for which the three short horizontal line segments indicate upper limits. All other data shown is taken directly from Fig. 11 of Gies et al. (2002). The meaning of the other symbols is given in Sec. 3.1 in the text. The spectral flux distribution of a reddened blackbody acceptably represents the observations in the visible. Fits with $T = 72,000$, 49,000, 45,000, and 21,000 K and $A_V = 8.4$, 8.2, 7.8, and 7.8 are shown as dotted, dashed, dot-dash, and solid lines, respectively.

162.5 d (precession) phase at the start of each observation is also given there. Observations 014 and 015 included multiple exposures in each filter and extended over 35 ks and 115 ks, respectively. The data were reduced using the standard *Swift* analysis programs (HEASoft 6.0).

3. RESULTS

3.1. *Photometry*

Figure 1, based on Fig. 11 of Gies et al. (2002), shows previously observed fluxes from SS433 in the optical and ultraviolet. The diamonds and squares are taken from Wagner (1986) for the bright and faint states of SS433 in the visible. The 2σ upper limits below 1700 Å are from Gies et al. (2002). The error bars at 2770 Å give the maximum and minimum fluxes reported by Dolan et al. (1997) using *HST*/HSP. The spectral flux distribution of a reddened blackbody acceptably represents the observations in the visible.

The mean flux at each epoch of observation (cf. Table 2) is shown in Fig. 1 in each UVOT bandpass. These fluxes agree with previous observations in the visible, and confirm the excess flux detected in the UV by Dolan et al. (1997). The mean flux at 1880 Å is detected at the 12σ level of significance in observation 015. It lies more than 20 times above the reddened blackbody spectral flux distribution extrapolated from the optical. No flux is detected in the UVM2 bandpass at 2170 Å, the wavelength of maximum interstellar absorption; the error bars shown are 2σ upper limits.

3.2. *Variability*

The mean flux in the five UV and optical bandpasses in which we detected the source varied from observation to observation, as expected for SS433. Historically, a bright state of SS433 occurs at precession phase 0.8 ± 0.05 (near maximum redshift separation of the two sets of emission lines) at the binary phase of greatest elongation ($\varphi = 0.3 \pm 0.15$) and a faint state occurs when photometric eclipse occurs, especially when the accretion disk around the X-ray source is nearly edge-on ($\psi = 0.27 \pm 0.1$) (Panferov et al. 1997). The lowest flux in the V bandpass was detected in observation 002, during photometric eclipse. Only an upper limit on the flux in the UVW2 bandpass was obtained at this epoch. (Observations in the other bandpasses were not made at this epoch.)

Variability of SS433 over a timescale of minutes has been reported in the optical (Zwitter et al. 1991; Revnivtsev et al. 2004; Cherepashchuk et al. 2005). Observations 013A and 013B, taken ~ 1.5 h apart, suggest that the far UV flux varies on a time scale of hours. We therefore monitored the source at ~ 90 min intervals over 0.4 d in observation 014 and over 1.3 d in observation 015 to investigate UV variability on this time scale. The fluxes from SS433 during these two observations in the UV and optical bandpasses and in the $0.2 - 10$ keV bandpass are shown as a function of time in Fig. 2. The flux density is variable on a time scale of hours in all six bandpasses. The increase in flux density occurring at JD 2453917.6 is correlated in the optical, UV, and X-ray bandpasses, rising to a

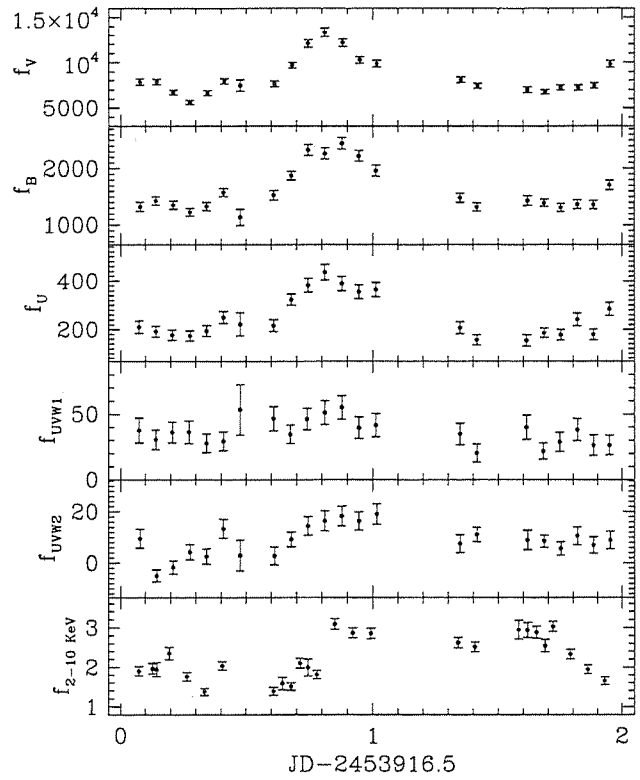

FIG. 2.— The flux density in μJy of SS433 during observations 014 and 015. The five UVOT bandpasses in which the source was detected are shown, along with the simultaneous 0.2-10 keV flux from the XRT.

maximum over a timescale of $\sim$ 10 ks. The flux density then decreases to its starting value over the next 40 ks in the optical and UV bandpasses. The X-ray flux density remains elevated for $\sim$ 70 ks after the X-ray maximum before decreasing to its pre-maximum value.

The additional flux appearing in each bandpass at the time of maximum flux density increases monotonically with frequency from $\sim$ 40% of the quiescent flux in the V bandpass to $\sim$ 75%, $\sim$ 180%, $\sim$ 250%, and $\sim$ 300% of the quiescent flux in the B, U, UVW1, and UVW2 bandpasses. The increase in the X-ray bandpass is $\sim$ 200% of the flux before and after maximum.

The X-ray spectrum we observed between $0.2 - 10$ keV during observation 015 is acceptably represented by the absorbed power law type of spectrum given in eqn. [1]. The minimum χ^2 spectral fit to our data has photon spectral index -1.52 ± 0.04 and $N_H = 6.4 \pm 0.3 \times 10^{21}$ cm^{-2}.

4. DISCUSSION

A luminosity component in addition to the reddened blackbody component that dominates the emission in the visible is clearly present in the far UV spectrum of SS433. This far UV component extends into the visible, as shown by the correlated variability we detected in the UV and optical bandpasses during observations 014 and 015. The reddened blackbody component dominates in the optical and near UV, however; the fractional contribution to the luminosity of the variability ascribed to the far UV component decreases monotonically with frequency into the optical.

Based on their correlated variability, the far UV component also extends into the soft X-ray region, but the power law continuum component must dominate there. Marshall et al. (2002) note that the continuum model they fit to their data at higher energies falls below the observed spectrum at wavelengths $>$ 7 Å (cf. their Fig. 7). We suspect that this additional luminosity may arise from the same component we detect in the far UV. The absorbed X-ray spectrum given by eqn. [1] extrapolated to 1880 Å lies two orders of magnitude below the flux we detect in the UVW2 bandpass.

The similarity between the jet plus accretion disk geometry of SS433 and that present in OVV quasars has led to SS433 being referred to as a microquasar (e.g., Cherepashchuk et al. 2003; Charles et al. 2004). We note that a luminosity component in the far UV in addition to those present in the optical and UV has been detected in the OVV quasar 3C345 (Dolan et al. 1994). The far UV component in 3C345 is produced by optically thin synchrotron radiation. A similar origin of the far UV component in SS433 would require its emission to be significantly polarized.

The location of the far UV component in the binary system can be determined by monitoring its flux as a function of 13 d and 162.5 d periods. In particular, if the far UV component is eclipsed near superior conjunction of the X-ray source, it must originate near the compact object itself, or at the base of the jets. The only non-detection of SS433 at 1880 Å occurred during photometric eclipse (observation 002), but the upper limit on the flux density at that epoch can not rule out a flux consistent with that observed at other times in the UVW2 bandpass.

5. CONCLUSIONS

A luminosity component in addition to those previously detected in the optical and X-ray regions must exist in the far UV spectrum of SS433.

We acknowledge assistance from the *Swift* team, especially Neil Gehrels and Sally Hunsberger for approving and scheduling the observations, and we thank Doug Gies for providing the data to reproduce Fig. 11 from Gies et al. (2002).

REFERENCES

Brinkman, W., Kawai, N., Matsuoka, M., & Fink, H. H. 1991, A&A, 241, 112

Burrows, D. N., et al. 2005, Sp. Sci. Rev., 120, 165

Charles, P. A., Barnes, A. D., Casares, J., Clark, J. S., Clarkson, W. I., Harlaftis, E. T., Hynes, R. I., Marsh, T. R., & Steeghs, D. 2004, RevMexAA, 20, 50

Cherepashchuk, A. M. 1981, MNRAS, 194, 761

Cherepashchuk, A. M., Sunyaev, R. A., Seifina, E. V., Panchenko., I. E., Molkov, S. V., & Postnov, K. A. 2003, A&A, 411, L441

Cherepashchuk, A. M., et al. 2005, A&A, 437, 561

Dolan, J. F., Boyd, P. T., Wolinski, K. G., Smith, P. S., Impey, C. D., Bless, R. C., Nelson, M. J., Percival, J. W., Taylor, M. J., Elliot, J. L., Robinson, E. L., & van Citters, G. W. 1994, ApJ, 432, 560

Dolan, J. F., Boyd, P. T., Fabrika, S., Tapia, S., Vychkov, V., Panferov, A. A., Nelson, M. J., Percival, J. W., van Citters, G. W., Taylor, D. C., & Taylor, M. J. 1997, A&A, 327, 648
Gehrels, N., et al. 2004, ApJ, 611, 1005
Gies, D. R., McSwain, M. M., Riddle, R. L., Wang, Z., Wiita, P. J., & Wingert, D. W. 2002, ApJ, 566, 1069
Goranskii, V. P., Esipov, V. F., & Cherepashchuk, A. M. 1998, Astr. Rep., 42, 209
Hjellming, R. N., & Johnston, K. J. 1981, Nature, 290, 100
Kotani, T., Kawai, N., Matsuoka, M., & Brinkman, W. 1996, PASJ, 48, 619
Margon, B. 1984, ARAA, 22, 507
Margon, B., & Anderson, S. F. 1989, ApJ, 347, 448
Marshall, F. E., Swank, J. H., Boldt, E. A., Holt, S. S., & Serlemitsos, P. J. 1979, ApJ, 230, L145
Marshall, H. L., Canizares, C. R., & Schultz, N. R. 2002, ApJ, 564, 941
Neill, A. E., Lockhart, T. G., & Preston, R. A. 1981, ApJ, 250, 248
Panferov, A. A., Fabrika, S. N., & Rakhimov, V. Y. 1997, Astr. Rep., 74, 392
Revnivtsev, M., Burenin, R., Fabrika, S., Postnov, K., Bikmaev, I., Pavlinsky, M., Sunyaev, R., Khamitov, I., & Aslan, Z. 2004, A&A, 424, L5
Roming, P. W. A., et al. 2005, Sp. Sci. Rev., 120, 95
Stephenson, C. B., & Sanduleak, N. 1977, ApJS, 33, 459
Vermeulen, R. C., Schilizzi, R. T., Spencer, R. E., Romney, J. D., & Fejes, I. 1993, A&A, 270, 177
Wagner, R. M. 1986, ApJ, 308, 15
Zwitter, T., Calvani, M., & D'Odorico, S. 1991, A&A, 251, 92